

Single photon emitters in exfoliated WSe₂ structures.

M. Koperski,^{1,2} K. Nogajewski,¹ A. Arora,¹ J. Marcus,³ P. Kossacki,^{1,2} and M. Potemski¹

¹*Laboratoire National des Champs Magnétiques Intenses, CNRS-UJF-UPS-INSA, 25 Rue des Martyrs, 38042 Grenoble, France*

²*Institute of Experimental Physics, Faculty of Physics, University of Warsaw, Hoża 69, 00-681 Warsaw, Poland*

³*Institut Néel, CNRS-UJF, BP 166, 38042 Grenoble, France*

Crystal structure imperfections in solids often act as efficient carrier trapping centers which, when suitably isolated, act as sources of single photon emission. The best known examples of such attractive imperfections are well-width or composition fluctuations in semiconductor heterostructures [1, 2] (resulting in a formation of quantum dots) and coloured centers in wide bandgap (e. g., diamond) materials [3–5]. In the case of recently investigated thin films of layered compounds, the crystal imperfections may logically be expected to appear at the edges of commonly investigated few-layer flakes of these materials, exfoliated on alien substrates. Here, we report on comprehensive optical microspectroscopy studies of thin layers of tungsten diselenide, WSe₂, a representative semiconducting dichalcogenide with a bandgap in the visible spectral range. At the edges of WSe₂ flakes, transferred onto Si/SiO₂ substrates, we discover centers which, at low temperatures, give rise to sharp emission lines (100 μeV linewidth). These narrow emission lines reveal the effect of photon antibunching, the unambiguous attribute of single photon emitters. The optical response of these emitters is inherently linked to two-dimensional properties of the WSe₂ monolayer, as they both give rise to luminescence in the same energy range, have nearly identical excitation spectra and very similar, characteristically large Zeeman effects. With advances in the structural control of edge imperfections, thin films of WSe₂ may provide added functionalities, relevant for the domain of quantum optoelectronics.

Investigations of thin layers of semiconducting transition metal dichalcogenides (TMDs) are driven by scientific curiosity (to uncover the properties of a new class of two-dimensional systems with unconventional electronic bands) and by their possible new functionalities arising from using a valley degree of freedom in optoelectronic devices [6]. Typically for the family of semiconducting TMDs, a one-molecule-thick layer of WSe₂ is known to display a robust photo-luminescence [7]. This is due to its direct bandgap semiconductor structure in contrast to the indirect bandgap structure of WSe₂ multilayers. Indeed, when increasing the number of layers, the photoluminescence (PL) of few-layer WSe₂ is progressively quenched and red shifted, and becomes practically un-

detectable in sufficiently thick layers [7]. Optical studies of WSe₂ layers are routinely performed on flakes exfoliated from bulk material and transferred onto Si/SiO₂ substrates. Such structures are also the objects of this work.

Optical-microscope images of two selected WSe₂ flakes are shown in Fig. 1a and 1d. A large part of the flake shown in Fig. 1a is identified as a monolayer, attached to a thicker WSe₂ film. When this flake is scanned with micro-PL spectra at low temperatures, the majority PL response of the WSe₂ monolayer exhibits a familiar form, known from literature [8]. As shown in Fig. 1c, the emission spectrum of the WSe₂ monolayer is composed of several, rather broad peaks (~20 meV linewidth). This spectrum is characteristic of an n-type WSe₂ monolayer [8] (unintentional doping in our case). The upper energy peak (at ~1.75 eV) is commonly attributed to a direct, free exciton resonance; the subsequent lower energy peaks are assigned to charged and bound (localized) excitons [9]. The contour image of the WSe₂ monolayer is clearly reproduced with mapping the intensity of the free exciton peak (see Fig. 1b). Interestingly enough, there exist specific spots on this flake at which the broad PL spectrum from the bulk of the WSe₂ monolayer tends to be replaced by a series of sharp (100 μeV linewidth) emission lines (see Fig. 1c). These narrow line emitting centers (NLECs) are located at the edge of the WSe₂ flake. This is shown with photoluminescence mapping of the intensity of one of the well spectrally-resolved narrow emission lines (see Fig. 1b). Markedly, the presence of NLECs is not only a property of the WSe₂ monolayer. In Fig. 1d - 1f the optical microscope image, the photoluminescence maps and spectra measured at selected spots are presented for a thick WSe₂ flake. Its thickness varies between 10 and 15 nm (6 - 9 monolayers), as estimated from AFM measurements on its different parts. Here, we show the presence of spots giving sharp emission lines, located again at the edges but, this time, of a rather thick WSe₂ flake. The characteristic NLECs have also been seen in a number of other WSe₂ flakes. Every time the NLECs are found at the flake edges and sharp emission lines always appear in the spectral range which overlaps with the broad emission band of charged and localized excitons of the WSe₂ monolayer. Studying the NLECs associated with thicker WSe₂ flakes is advantageous as the emission from the bulk of these flakes is suppressed and sharp edge-emission lines are better resolved.

Single isolated centers in solids often act as efficient,

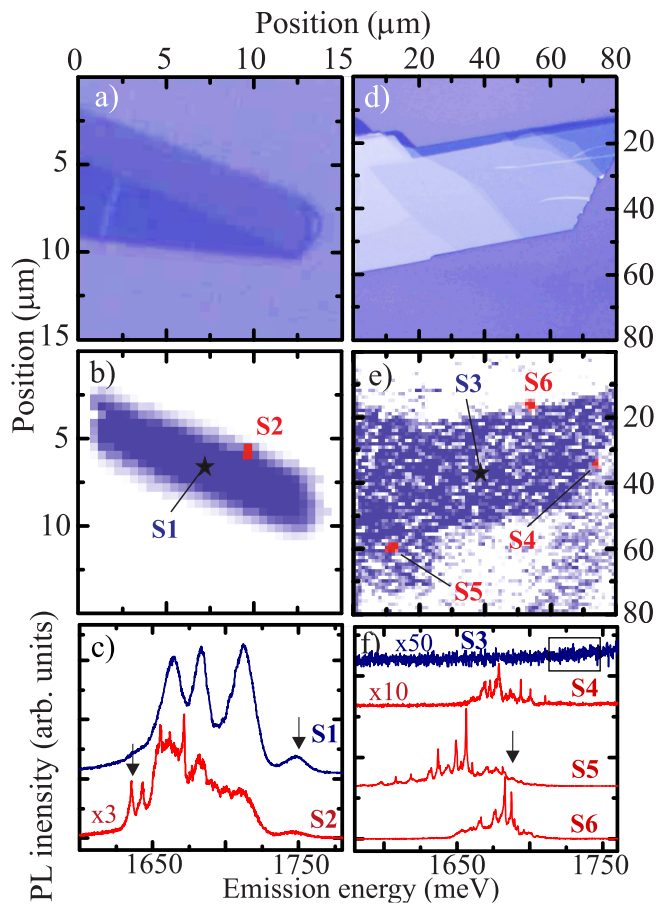


FIG. 1: **Images and scanning μ PL spectroscopy on WSe_2 layers, revealing narrow line emission centers at the edges of flakes deposited on Si/SiO_2 substrates.** **a**, Optical microscope images of a thin WSe_2 flake. A large part of this flake consists of a WSe_2 monolayer whose image is reproduced in **b**, with a contour plot (violet contrast) of the intensity of the μ PL detected at the selected emission energy of $E \sim 1.75$ eV (free-exciton resonance of a WSe_2 monolayer). **c**, μ PL spectra measured from two selected spots of the WSe_2 monolayer, S1 and S2. The PL at the central spot (S1) is a known spectrum of the WSe_2 monolayer and indeed characteristic of the majority of spots on the surface of our monolayer. Sharp emission lines are seen on the top of the rather broad S1-like spectrum at specific spots (e. g., S2,) located at the edges of the flake. The location of S2 is shown in **b**, with a contour plot (red contrast) of the intensity of the sharp line observed at $E = 1.636$ eV. The thick flake of WSe_2 illustrated with the optical-microscope image in **d**, shows a suppressed PL but nevertheless its image can be reproduced in the course of μ PL scanning experiments as shown by the contour plot with violet contrast in **e**, which represents the intensity map of scattered light detected in the energy interval 1.71-1.75 eV. Shown in **f**, the narrow-line emission spectra, S4-S5, are found at specific edge locations of the thick WSe_2 flake, as illustrated in **e** with the contour plot (red contrast) of the PL monitored at $E = 1.687$ eV.

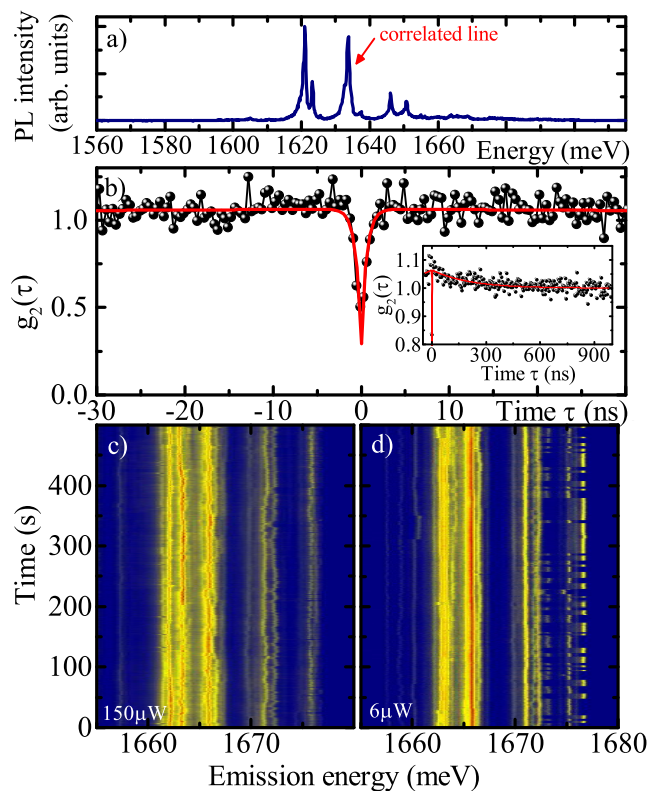


FIG. 2: **Narrow line PL centers as sources of single photon emission.** **a**, Narrow line emission spectrum detected at the micro-spot located at the edge of one of the thick WSe_2 flakes. **b**, Photon coincidence correlation, $g_2(\tau)$, which displays the effect of photon antibunching, with a characteristic time of ~ 600 ps, for one of the narrow emission lines marked in **a**. A weak bunching effect on a longer time scale (200 ns), shown in the inset, is likely caused by temporal jittering of the center of the line. **c**, Two sets of narrow line emission spectra, recorded one after another, with 100 ms resolution, measured under two different powers of laser excitations (150 and $6 \mu\text{W}$), which demonstrate the line jittering effects being less pronounced at lower excitation powers.

high-fidelity single photon emitters [10]. The NLECs at the edges of WSe_2 flakes exhibit this property as well. This is illustrated in Fig. 2 with results of single photon correlation measurements performed on one of the selected sharp emission lines. Photon antibunching in the autocorrelation function is clear. The characteristic coincidence time in the auto-correlation function, which yields the upper bound for the lifetime of the emitting state, is estimated to be about 600 ps for this particular line and reaches up to a few nanoseconds for other investigated lines. The NLECs at the edges of WSe_2 flakes appear to be overall robust on a long time scale and survive many temperature cycles (room to helium temperature) including prolonged exposures to ambient (air) conditions. Nevertheless, our NLECs show clear fluctuation effects on a short time scale: jittering of centers of lines, of the order of the linewidth, on a millisecond time scale as well as larger jumps of lines on a time scale of seconds

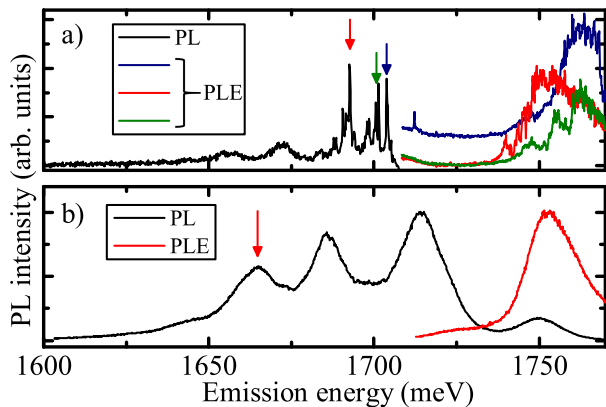


FIG. 3: **Absorption resonances of narrow-line-emission centers and of a 2D WSe₂ monolayer.** PL excitation spectra measured in the range available with a Ti:Sapphire laser for, **a**, three selected narrow PL lines associated with the edge of the thick WSe₂ flake, and of, **b**, the localized exciton band of the 2D WSe₂ monolayer. The detection energies are shown with arrows. The approximately coinciding absorption resonances underline a link between the electronic states of the edge emission centers and of the WSe₂ monolayer.

(see Fig. 2c). Stability is improved when decreasing the power of the laser excitation. This behavior is characteristic of many other single photon emitters, such as, for example semiconductor quantum dots, and it is commonly associated with fluctuations of electric charge in the surrounding of the emitting center [11].

Having established the single-photon-emitter character of NLECs at the edges of WSe₂ flakes, we now focus more on their optical properties. The first task is to identify their absorption resonances. The PL-excitation spectra of three selected narrow lines (of the NLEC at the edge of the thick WSe₂ flake) are presented in Fig. 3a. Each of these lines resonates in a slightly different energy range, though all three absorption resonances overlap quite well with the characteristic absorption band of the WSe₂ monolayer film (see Fig. 3b). This approximate coincidence highlights the link between the electronic band structures of our NLECs and of the WSe₂ monolayer; the statement being also applied to the case when NLECs are attached to thick WSe₂ films.

The fact that electronic structure of our NLECs may originate from that of the WSe₂ monolayer is further supported by the magneto-PL measurements. These experiments have been carried out in a large range of magnetic fields (up to 29T), in the Faraday configuration, and σ_+ and σ_- circular polarization components of the emitted light were resolved (by inverting the direction of the magnetic field while passing the emitted light through a fixed ensemble of a linear polarizer and a $\lambda/4$ plate). In Fig. 4, we compare the magneto-PL response of the WSe₂ monolayer film with that of the NLEC attached to this layer. The details of these data remain to be thoroughly analyzed. Here we focus on one of their prominent features,

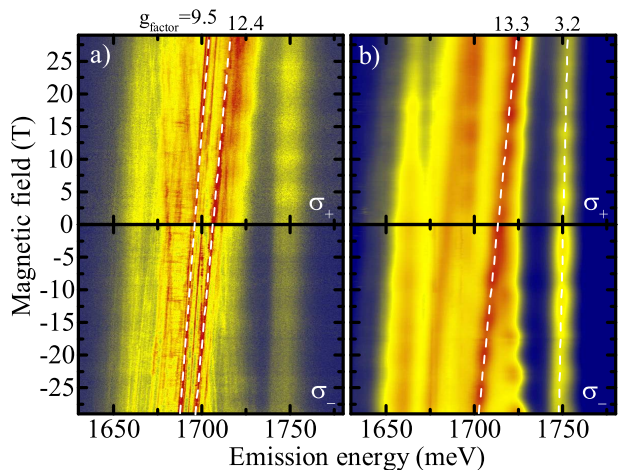


FIG. 4: **Narrow line emission centers and a 2D WSe₂ monolayer in a magnetic field.** Intensity contour plots of micro-magneto-PL spectra measured in the Faraday configuration: **a**, from the edge spot giving rise to sharp emission lines and, **b**, from the center of the WSe₂ monolayer. The top and bottom panels correspond to the spectra, resolved in circular polarizations σ_+ and σ_- , respectively. The characteristic amplitude of the splitting of the emission lines into σ_+ and σ_- components (see white dashed white traces) is expressed in terms of g -factors (splitting = $g\mu_B B$). Note, the anomalously large but, at the same time, similar splitting for the narrow lines and for one of the broad PL peaks (due to a charged exciton) of the monolayer. The oscillations of the PL intensity with the magnetic field visible in the spectra are due to the use of fiber optics in our experiments (see Methods).

relevant for this work. Remarkably, we observe a striking resemblance in the amplitude of the σ_+/σ_- splitting (Zeeman splitting) for the charged exciton of the two-dimensional monolayer and for the narrow emission lines, in that both show an anomalously large Zeeman effect. The characteristic amplitude of the g -factor (splitting = $g\mu_B B$) for charged excitons is $g \sim 13$ and similarly large values ($g \sim 9 - 12$) are found for the emission lines of our NLECs. The difference in the amplitude of the Zeeman splitting for the neutral ($g \sim 3.2$) and charged exciton of the WSe₂ monolayer remains a puzzle as already reported in Ref. 12. An overall large Zeeman effect in WSe₂ is likely due to a strong, spin-orbit interaction in this material. This issue remains to be clarified, but the similarity between Zeeman effects found for the WSe₂ monolayer and for the NLECs is an additional indication that the matrix of our NLECs might be formed out of the WSe₂ monolayer.

A firm identification of NLECs seen at the edges of the WSe₂ flakes is an obvious challenge. Our working hypothesis is that these NLECs consist of nano-sized, lateral fragments (nano-flakes) of a WSe₂ monolayer, which are apparently formed at the edges of exfoliated flakes of monolayers as well as WSe₂ multilayers. Notably, the appearance of monolayer nano-flakes at the edges of thick multilayers may not be surprising as it is quite character-

istic for the exfoliation technique that even large monolayers can be found on the sides of thick flakes of various exfoliated/transferred materials (e.g. graphene) [13]. Nonetheless, these nano-flakes are usually isolated and display relevant quantum confinement effects, what accounts for the observation of narrow and single-photon emission lines. As such, our NLECs can be seen as quantum dots made of the WSe₂ monolayer, objects similar to those extensively studied in conventional semiconductor structures [14]. The resemblance of the optical responses of the WSe₂ monolayer and the NLECs (similar emission spectral range, similar absorption resonances and Zeeman splittings) favors these claims. Since the spectral range of sharp emission line covers the PL band of trions and/or bound exciton of the WSe₂ monolayer, the nano-flakes should act as efficient traps for the electric charge; the observed sharp emission lines must then be due to charged excitonic complexes as well. The characteristic, temperature-activated broadening of NLEC spectra (not shown) resembles effects found in semiconductor quantum dots (acoustic phonon broadening [15]) and additionally supports the analogies invoked above.

The monolayer nano-flake (quantum dot) scenario for our NLECs is plausible but obviously needs further clarifications/work and other hypotheses should be discussed at present. In this light, our unsuccessful efforts to observe any signature of a sequential (cascaded) emission in photon cross-correlation measurements between any pair of the NLEC lines tested are disappointing from the point of view of the quantum dot scenario. This sequential emission, a prominent example of which is the biexciton - exciton cascade, is a distinct feature of semiconductor quantum dots (and nanocrystals) [16]. On the other hand, this feature is absent for all other single photon-emitters, such as organic molecules, colored centers in crystals [10] and also individual carbon nanotubes [17]. The possibility that our NLECs are due to an insufficiently clean exfoliation procedures, as a result of which some organic molecules are attached and functionalized at the edges of WSe₂ flakes, is unlikely. This is because of the overall robustness of our NLECs and the anomalously large Zeeman effect (unexpected for organic, carbon based molecules with a small spin-orbit interaction). So far, all our efforts to localize the NLECs with AFM measurements have failed, but this is perhaps not surprising due to the insufficient spatial resolution of this technique. Instead, however, we have systematically observed that the thickness of our WSe₂ films is slightly enhanced at the side of the flake. This may also signify the effect of curling of the WSe₂ layer at the flake edges [18], but suggesting the edge defects in form of a WSe₂ nanotube [19] is highly speculative. Nevertheless, the latter, as well as any other defect evoking hypothesis, is to be tested in the future. This, we believe, can be efficiently done with scanning tunneling microscopy/spectroscopy as our NLECs appear on an open surface and WSe₂ flakes can be suitably transferred onto a conducting (e. g. graphene) substrates.

Concluding, we have identified single photon emitting centers which are located at the edges of WSe₂ flakes (mono- and multi-layers) exfoliated onto Si/SiO₂ substrates. The characteristic spectra of these centers, seen at low temperatures (≤ 20 K), are composed of a series of sharp emission lines which clearly reveal the effect of photon-antibunching. In a number of aspects, the optical response of the sharp emission lines resembles that of the WSe₂ monolayer: overlapping spectral emission range, coinciding absorption resonances and similar anomalously large Zeeman splittings. With these observations, the single photon emitters reported here are recognized as nano-flakes (quantum dots) of the WSe₂ monolayer, located at the edges of conventionally studied WSe₂ films. Our findings may open a new field of quantum optoelectronics studies of thin layers of semiconducting transition metal dichalcogenides. When setting up this manuscript, we have noticed another paper [20] reporting findings similar to ours.

Methods

The samples used in the experiments were prepared by mechanical exfoliation of bulk WSe₂. We followed the procedure which has recently been demonstrated in Ref. 21. For thinning down the flakes we used F07 acrylic tape from Microworld and for transferring them onto a target substrate (a piece of undoped silicon wafer with an 86 nm-thick layer of thermally grown silicon dioxide on top), polydimethylsiloxane-based elastomeric films from Gel-Pak. All Si/SiO₂ substrates had been photolithographically equipped with Ti/Au alignment markers to facilitate locating the flakes under different optical setups and ashed with oxygen plasma shortly before exfoliation to clean and activate their surface. The AFM characterization of the flakes was performed in a tapping mode with the aid of a Veeco Dimension 3100 microscope.

The optical studies were carried-out in μ PL setups. The diameter of the laser beam was typically about 1 μ m. The spectra were resolved with a 50 cm monochromator with a 600 or 1800 g/mm grating and detected with a charge coupled device (CCD) camera. The magneto-optical studies in the Faraday configuration were performed in a resistive magnet supplying magnetic fields up to 29T. In this setup the sample was mounted on an x-y-z piezo-stage allowing the positioning of the sample with submicrometer precision. Optical fibers were employed in the set-up, to transfer the excitation light (from tunable Ti:Sapphire laser) and to collect the PL signal. The μ PL setup was placed in a probe, filled with helium exchange gas and cooled down to 4.2 K. A $\lambda/4$ waveplate and a linear polarizer were aligned as a circular polarizer in front of the entrance of the detection fiber, in order to obtain circular polarization resolution. Due to the presence of optical fibers, the magnetic-field induced rotation of the linear polarization angle (Faraday effect) introduced oscillations of the emission intensity observed in the magnetic field evolution of the PL spectrum.

Photon correlation measurements were performed in a

Hanbury-Brown and Twiss configuration with an argon laser (488.0 nm) excitation. Avalanche photodiodes were used for photon detection, with a temporal resolution of about 300 ps. The sample resided in a flow cryostat at a temperature of 4.2K. The correlation function obtained in the experiments was described with the following formula:

$$g_2(\tau) = 1 - A_1 * \exp\left(-\left|\frac{\tau}{t_1}\right|\right) + A_2 * \exp\left(\left|\frac{\tau}{t_2}\right|\right) \quad (1)$$

where t_1 is a characteristic time for the photon antibunching, t_2 is a characteristic time of the long-timescale bunching, A_1 is the antibunching depth and A_2 is the bunching amplitude. In case of the example correla-

tion function shown here, the depth of the antibunching was equal to $A_1 = 0.77 \pm 0.08$, which signifies that the emitter is a single photon source. The characteristic time was $t_1 = 0.61 \pm 0.08$ ns. The time of the long-time bunching was $t_2 = 204 \pm 22$ ns with a small amplitude $A_2 = 0.064 \pm 0.004$.

Acknowledgments

The authors thank M.L. Sadowski for valuable discussions and I. Breslavetz for technical assistance, and acknowledge the support from the European Research Council (MOMB project No. 320590), the EC Graphene Flagship project (No. 604391) and the NCN "Harmonia" programme.

-
- [1] Reed, M. A., Randall, J. N., Aggarwal, R. J., Matyi, R. J., Moore, T. M., Wetsel, A. E., *Observation of discrete electronic states in a zero-dimensional semiconductor nanostructure*, Phys. Rev. Lett. **60**, 535 (1988).
- [2] Michler, P., Kiraz, A., Becher, C., Schoenfeld, W. V., Petroff, P. M., Zhang, L., Hu, E., Imamoglu, A., *A Quantum Dot Single-Photon Turnstile Device*, Science **290**, 2282 (2000).
- [3] Gruber, A., Drabenstedt, A., Tietz, C., Fleury, L., Wrachtrup, J., von Borczyskowski, C., *Scanning Confocal Optical Microscopy and Magnetic Resonance on Single Defect Centers*, Science **276**, 2012 (1997).
- [4] Brouri, R., Beveratos, A., Poizat, J-P., Grangier, P., *Photon antibunching in the fluorescence of individual color centers in diamond*, Opt. Lett. **25**, 1294 (2000).
- [5] Mizuochi, N., Makino, T., Kato, H., Takeuchi, D., Ogura, M., Okushi, H., Nothaft, M., Neumann, P., Gali, A., Jelezko, F., Wrachtrup, J., Yamasaki, S., *Electrically driven single-photon source at room temperature in diamond*, Nature Photonics **6**, 299 (2012).
- [6] Wang, Q. H., Kalantar-Zadeh, K., Kis, A., Coleman, J. N., Strano, M. S., *Electronics and optoelectronics of two-dimensional transition metal dichalcogenides*, Nature Nanotechnology **7**, 699 (2012).
- [7] Zhao, W., Ghorannevis, Z., Chu, L., Toh, M., Kloc, C., Tan, P-H., Eda, G., *Evolution of Electronic Structure in Atomically Thin Sheets of WS₂ and WSe₂*, ACS Nano **7**, 791 (2013).
- [8] Jones, A. M., Yu, H., Ghimire, N. J., Wu, S., Aivazian, G., Ross, J. S., Zhao, B., Yan, J., Mandrus, D. G., Xiao, D., Yao, W., Xu, X., *Optical generation of excitonic valley coherence in monolayer WSe₂*, Nature Nanotechnology **8**, 634, (2013).
- [9] Wang, G., Bouet, L., Lagarde, D., Vidal, M., Balochi, A., Amand, T., Marie, X., Urbaszek, B., *Valley dynamics probed through charged and neutral exciton emission in monolayer WSe₂*, Phys. Rev. B **90**, 075413 (2014).
- [10] Lounis, B., Orrit, M., *Single-photon sources*, Rep. Prog. Phys. **68**, 1129 (2005).
- [11] Pietka, B., Suffczyński, J., Goryca, M., Kazimierzczuk, T., Golnik, A., Kossacki, P., Wyszomolek, A., Gaj, J. A., Stepniewski, R., Potemski, M., *Photon correlation studies of charge variation in a single GaAlAs quantum dot*, Phys. Rev. B **87**, 035310 (2013), and references therein.
- [12] Srivastava, A., Sidler, M., Allain, A. V., Lembke, D. S., Kis, A., Imamoglu, A., *Valley Zeeman Effect in Elementary Optical Excitations of a Monolayer WSe₂*, Preprint at <http://arxiv.org/abs/1407.2624> (2014).
- [13] Blake, P., Hill, E. W., Castro Neto, A. H., Novoselov, K. S., Jiang, D., Yang, R., Booth, T. J., Geim, A. K., *Making graphene visible*, Appl. Phys. Lett. **91**, 063124 (2007).
- [14] Yamamoto, Y., Santori, C., Solomon, G., Vuckovic, J., Fattal, D., Waks, E., Diamanti, E., *Single photons for quantum information systems*, Progress in Informatics **1**, 5-37 (2005)
- [15] Besombes, L., Kheng, K., Marsal, L., Mariette, H., *Acoustic phonon broadening mechanism in single quantum dot emission*, Phys. Rev. B **63**, 155307 (2001).
- [16] Moreau, E., Robert, I., Manin, L., Thierry-Mieg, V., Gérard, J. M., Abram, I., *Quantum Cascade of Photons in Semiconductor Quantum Dots*, Phys. Rev. Lett. **87**, 183601 (2001).
- [17] Högele, A., Galland, C., Winger, M., Imamoglu, A., *Photon Antibunching in the Photoluminescence Spectra of a Single Carbon Nanotube*, Phys. Rev. Lett. **100**, 217401 (2008).
- [18] Huang, J. Y., Ding, F., Yakobson, B. I., Lu, P., Qi, L., Li, J., *In situ observation of graphene sublimation and multi-layer edge reconstructions*, PNAS **106**, 10103-10108 (2009).
- [19] Natha, M., Rao, C. N. R., *MoSe₂ and WSe₂ nanotubes and related structures*, Chem. Commun. **21**, 2236-2237 (2001).
- [20] Srivastava, A., Sidler, M., Allain, A. V., Lembke, D. S., Kis, A., Imamoglu, A., *Optically Active Quantum Dots in Monolayer WSe₂*, Preprint at <http://arxiv.org/abs/1411.0025> (2014).
- [21] Castellanos-Gomez, A., Buscema, M., Molenaar, R., Singh, V., Janssen, L., van der Zant, H. S. J., Steele, G. A., *Deterministic transfer of two-dimensional materials by all-dry viscoelastic stamping*, 2D Mater. **1**, 011002 (2014).